RHGF-1/PDZ-RhoGEF and retrograde DLK-1 signaling drive neuronal remodeling on microtubule disassembly

Chun-Hao Chen[a], Albert Lee[b], Chien-Po Liao[a], Ya-Wen Liu[a], and Chun-Liang Pan[a,1]

[a]Institute of Molecular Medicine, College of Medicine, and [b]Department of Chemistry, National Taiwan University, Taipei 100, Taiwan

Edited by Yuh Nung Jan, Howard Hughes Medical Institute, University of California, San Francisco, CA, and approved October 7, 2014 (received for review June 3, 2014)

Neurons remodel their connectivity in response to various insults, including microtubule disruption. How neurons sense microtubule disassembly and mount remodeling responses by altering genetic programs in the soma are not well defined. Here we show that in response to microtubule disassembly, the *Caenorhabditis elegans* PLM neuron remodels by retracting its synaptic branch and overextending the primary neurite. This remodeling required RHGF-1, a PDZ-Rho guanine nucleotide exchange factor (PDZ-RhoGEF) that was associated with and inhibited by microtubules. Independent of the myosin light chain activation, RHGF-1 acted through Rho-dependent kinase LET-502/ROCK and activated a conserved, retrograde DLK-1 MAPK (DLK-1/dual leucine zipper kinase) pathway, which triggered synaptic branch retraction and overgrowth of the PLM neurite in a dose-dependent manner. Our data represent a neuronal remodeling paradigm during development that reshapes the neural circuit by the coordinated removal of the dysfunctional synaptic branch compartment and compensatory extension of the primary neurite.

axon retraction | axon regeneration | Rho signaling | DLK | microtubules

The connectivity of neuronal circuits is established first through a highly dynamic phase of addition or elimination of axon branches and synapses, followed by a maintenance phase in which axon and dendritic branches show remarkable stability during the lifetime of postmitotic neurons. Disruption of neuronal circuits elicits remodeling responses that eliminate dysfunctional neurites or synapses and may stimulate the regeneration of injured axons. To enable these remodeling responses, neurons need to sense the insults and signal to the effectors that execute either retraction or extension of the neuronal structures. A well-studied effector for neuronal remodeling is the dual leucine-zipper kinase DLK, whose activation is required for both Wallerian degeneration and axon regeneration after injury, depending on the species and contexts examined (1–4). The DLK protein level is primarily controlled by proteasomal turnover that depends on Highwire/RPM-1, a ubiquitin E3 ligase that targets DLK for degradation (5). The *Caenorhabditis elegans* DLK, DLK-1, is activated by calcium influx during axon injury that triggers the dissociation of an inhibitory DLK-1 isoform (6). A recent report suggests that *C. elegans dlk-1* is a direct transcriptional target of the FoxO transcription factor DAF-16 in axon regeneration (7). Despite the extensive characterization of DLK, little is known about how neurons sense various insults and translate them into DLK-activating signals.

Microtubules are a major neuronal cytoskeleton component that shapes and maintains synapses and axons (8, 9). Mutations in Ankyrin and α-spectrin, two membrane skeletal proteins that organize microtubules at presynaptic sites, triggered synaptic bouton shrinkage and axon terminal retraction at *Drosophila* neuromuscular junction, highlighting the central importance of microtubules in the maintenance of synapses and axon branches (10, 11). Recent studies in *C. elegans* showed that the microtubule minus end-binding protein PTRN-1/CAMSAP maintained synapse and neurite stability by stabilizing microtubule foci and promoting microtubule polymerization (12, 13). *ptrn-1* mutants showed signs of neuronal remodeling, with loss of the synaptic branch and overgrowth of the primary neurite in the PLM touch neuron (12). However, how microtubules coordinate structural stability and remodeling of neurons under insults remains incompletely understood. Genetic or pharmacologic ablation of microtubules in the *C. elegans* touch neurons reduced the expression of several touch neuron-specific genes through the activation of the DLK-1 MAPK pathway (14). Because DLK-1 is a major effector for neuronal remodeling, taken together, these studies raise the possibility that microtubule disruption drives neuronal remodeling through DLK-1 activation. How this is achieved at the molecular level remains unknown.

In this study, we report that in the *C. elegans* touch neurons, microtubules maintain axon branch stability by sequestering a microtubule-associated RhoGEF, RHGF-1. Microtubule loss caused by tubulin mutations released RHGF-1, which then induced synaptic and axon branch defects and neurite overextension by activating a retrograde DLK-1 signaling pathway. We propose that RHGF-1 functions to detect microtubule disruption, thus coupling microtubule disassembly to the activation of the conserved remodeling effector DLK-1 to clear the disabled axon branch compartment and promote excessive growth of the primary neuronal process.

Results

***C. elegans* Tubulins MEC-12 and MEC-7 Are Required for PLM Axon Branch Maintenance.** The bilaterally symmetric *C. elegans* PLM touch neurons extend an anterior process, which has a single collateral branch that forms chemical synapses with axons in the ventral nerve cord (Fig. 1*A*). Outgrowth of the PLM branch began during late embryogenesis and was complete by 10–12 h posthatching [late stage 1

Significance

Structural remodeling of neurons after insults to the nervous system includes retraction of the dysfunctional synaptic branches and growth of the primary neurites or new collateral branches. We find that genetic disruption of neuronal microtubules in *Caenorhabditis elegans* triggered structural remodeling through RHGF-1/RhoGEF, which is normally associated with and inhibited by microtubules. A conserved dual leucine zipper kinase, DLK-1, was activated by RHGF-1-dependent signaling, and activated DLK-1 was transported from distal neurite to the neuronal cell body, where it potentially altered genetic programs that enabled the destruction of injured synaptic branches and stimulated compensatory growth of the primary neurite. As microtubule, RhoGEF and DLK are conserved, the remodeling mechanisms described in this work could be a shared feature of both invertebrate and vertebrate nervous systems.

Author contributions: C.-H.C., A.L., and C.-L.P. designed research; C.-H.C., A.L., C.-P.L., Y.-W.L., and C.-L.P. performed research; C.-H.C., Y.-W.L., and C.-L.P. analyzed data; and C.-H.C. and C.-L.P. wrote the paper.

The authors declare no conflict of interest.

This article is a PNAS Direct Submission.

[1]To whom correspondence should be addressed. Email: chunliangpan@gmail.com.

This article contains supporting information online at www.pnas.org/lookup/suppl/doi:10.1073/pnas.1410263111/-/DCSupplemental.

larvae (L1)], followed by progressive enlargement of the presynaptic varicosities that were enriched in synaptic vesicles, active zone protein, mitochondria, and F-actin, marked by GFP::RAB-3, SYD-2::GFP, TOMM20::mCherry, and mCherry proteins fused to the filamentous actin-binding utrophin-calponin homology sequence (mCherry::utCH), respectively (Fig. 1*B*) (15). This region also opposed the postsynaptic sites of the glutamatergic interneurons (Fig. 1*C*). This constitutes part of the neuronal circuit that mediates accelerated forward movements on light touch stimulation on the posterior body wall of the animal (16).

To investigate genes required for the development of the PLM branch, we screened a few candidates by mutant analysis or RNAi (Dataset S1). We found that PLM neurons in the null mutants for the α-tubulin *mec-12* (17, 18) or the β-tubulin *mec-7* (*e1607* and *ok2152*, respectively) (17, 19) generated the synaptic branch similarly to the wild-type, but subsequently retracted it (Fig. 1 *D* and *F*), indicating that *mec-12* and *mec-7* are essential for PLM branch maintenance. These tubulin mutants also had progressively smaller PLM presynaptic varicosities (Fig. 1 *E* and *G*). This contrasts with the mutant for the ventral guidance gene *unc-6*/netrin, which showed nonprogressive PLM branch defects and suggested *unc-6* was required for the outgrowth, rather than the maintenance, of the PLM branch (Fig. 1*F* and Dataset S1). The *mec-12; mec-7* double mutants showed comparable PLM branch defects to those of the *mec-12* or *mec-7* single mutants, suggesting these two genes function in a common pathway (Fig. 1*H*). Touch neuron-specific expression of *mec-12* or *mec-7* rescued the PLM branch defects, confirming an autonomous role for these tubulins (Fig. 1*H*).

Treatment of wild-type animals with the microtubule-depolymerizing drug colchicine induced PLM branch retraction in a dose-dependent manner (Fig. S1*A*). Conversely, treatment of the tubulin mutants with taxol, which stabilizes microtubules, significantly rescued PLM branch defects (Fig. S1*B*), supporting a role for microtubules in maintaining the PLM axon branch. Of note, we found that it was critical to administer taxol at early larval stages before significant branch retraction ensued (Fig. S1*B*). Administration of taxol at L2 or later failed to show any rescue effects, whereas transient taxol treatment in L1 was sufficient to rescue a significant portion of branch retraction (Fig. S1*B*). This was striking, given that most *mec-12* or *mec-7* animals still retained the PLM branch at L2 (Fig. 1*F*). It raises the intriguing possibility that PLM branch defects in the tubulin mutants involve signaling events that commence early on microtubule loss.

In the wild-type, the PLM process stops behind the ALM soma, a phenomenon known as neurite tiling (20). Interestingly, in some *mec-12* and *mec-7* animals, the PLM process extended beyond the ALM soma or turned ventrally to contact axons in the ventral nerve cord (Fig. 1*I*). Occasionally, growth cones or end foot-like structures were visible at the distal PLM process of the tubulin mutants. Emergence of the overgrowth phenotype paralleled branch retraction in the PLM neuron (Fig. 1*J*). We confirmed that this overextension phenotype was also caused by a loss of *mec-12* and *mec-7* functions autonomously in the touch neurons (Fig. 1*K*). Taken together, microtubule disruption in the PLM triggers two

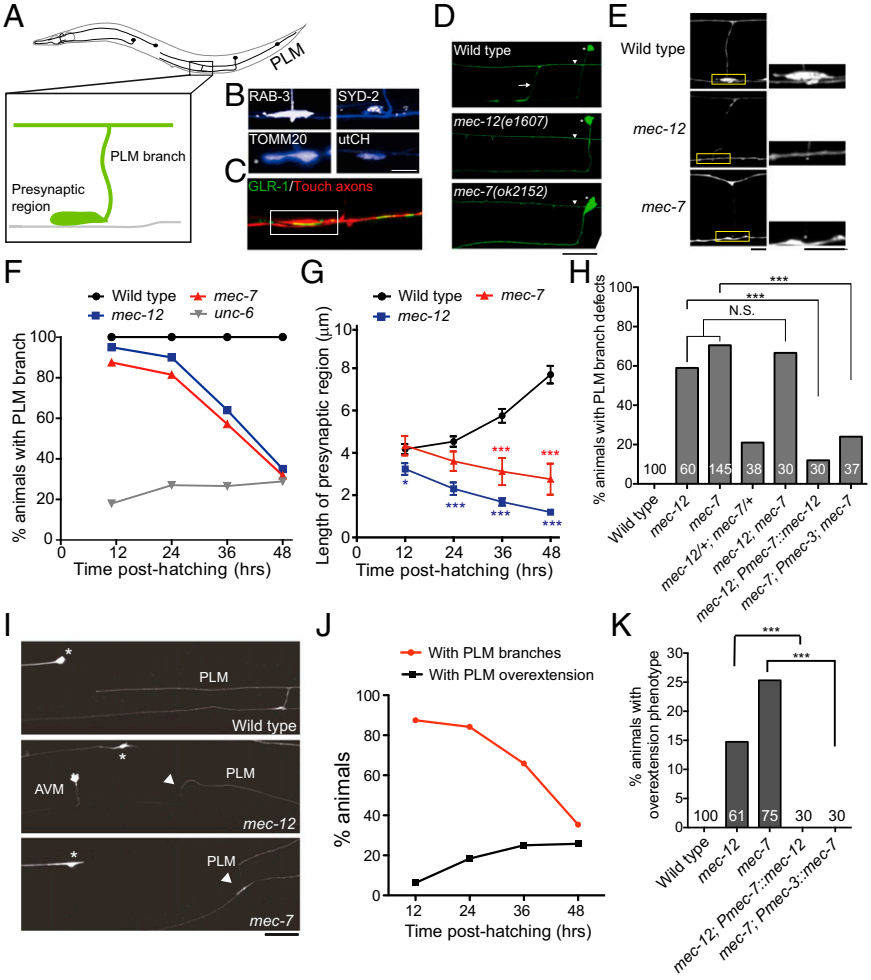

Fig. 1. *mec-12* and *mec-7* are essential for the PLM branch stability. (*A*) Schematic diagram of *C. elegans* touch neurons. Anterior is to the left. (*B*) The PLM presynaptic varicosities were enriched in synaptic vesicles, the active zone protein SYD-2, the mitochondria, and the synapse-specific F-actin. The PLM neurite was labeled by *zdIs5(Pmec-4::GFP)* or *jsIs973(Pmec-7::mRFP)* and pseudocolored in blue and synaptic markers in white. (Scale bar, 10 μm.) (*C*) Confocal image showing that the PLM presynaptic varicosities (red) opposed GLR-1 clusters (green) of the postsynaptic glutamatergic interneurons. (Scale bar, 5 μm.) (*D*) Confocal images of the PLM branch (arrow) in L4 larvae. Asterisks, PVM neurons; arrowheads, PLM processes. (Scale bar, 20 μm.) (*E*) The PLM presynaptic varicosities, visualized with *zdIs5(Pmec-4::GFP)*, at the L4 stage. Boxed regions were highlighted. (Scale bar, 10 μm.) (*F*) Quantification of animals with intact PLM branches at different larval stages. (*G*) The length of the PLM presynaptic varicosities at different larval stages. Error bar, SEM $^{**}P < 0.01$; $^{***}P < 0.001$, Mann–Whitney *U* test. (*H*) Quantification of L4 animals with PLM branch defects. *tm5083* and *e1507* were other null alleles for *mec-12* and *mec-7*, respectively. $^{***}P < 0.001$, two-proportion *z* test. N.S., not significant. (*I*) Confocal images of PLM neurite overextension in L4 larvae. Arrowheads, ventral migration of the PLM process tip to reach the ventral nerve cord; asterisks, ALM soma. (*J*) Quantification of PLM branch retraction and neurite overextension in *mec-7* animals at different larval stages. $n > 30$. (*K*) Quantification of L4 animals with PLM neurite overextension. $^{***}P < 0.001$, two-proportion *z* test.

NEUROSCIENCE

tightly coupled neuronal remodeling events: retraction of the synaptic branch and overextension of the primary neuronal process.

RHGF-1 Mediates Axon Branch Retraction and Neurite Overextension in the Tubulin Mutants. Studies in mammalian cells suggest that microtubule depolymerization leads to RhoA activation (21, 22), and RhoA activation has been shown to induce olfactory axon retraction in *Drosophila* (23). To explore whether Rho or related Rac signaling mediates PLM branch retraction on microtubule disruption, we knocked down most of the putative RhoGEFs in the *mec-7* mutant by feeding RNAi in a genetic background (strain: *sid-1; mec-7; uIs71[Pmec-18::sid-1]*) in which touch neurons are the only RNAi-sensitive cells (see *SI Materials and Methods*) (24, 25). We found that knockdown of two RhoGEFs, *rhgf-1* and *rhgf-2*, resulted in moderate but significant suppression of the branch defects of the *mec-7* mutant (Dataset S1). Because the *rhgf-2* null mutant was lethal, we focused on the genetic analysis of *rhgf-1*.

RHGF-1 is a multidomain protein that contains PDZ, RGS (regulator of G protein signaling), C1 (phorbol esters/diacylglycerol binding), DH (Dbl homology), and PH (pleckstrin homology) domains (Fig. 2*A*) (26, 27). The GTP exchange activity of RHGF-1 resides in the DH domain. Previous studies indicated that RHGF-1 participated in neurotransmitter release (26, 28). Consistent with its roles in the nervous system, *rhgf-1* was expressed in many neurons in *C. elegans*, including the PLM (Fig. 2*B*). Two available alleles, *ok880* and *gk217*, are in-frame deletions of the DH and the C1 domains, respectively (Fig. 2*A*) (26). We first tested *rhgf-1(ok880)* and found that it significantly suppressed synaptic defects and branch retraction (Fig. 2 *C* and *D*), as well as neurite overextension of the tubulin mutants (from 14–25% to 0–3%). The *rhgf-1(ok880)* mutant was also more resistant to branch defects induced by higher concentrations of colchicine (Fig. 2*E*). Expression of RHGF-1 in the touch neurons fully restored the branch defects of the *mec-7 rhgf-1(ok880)* or *mec-12; rhgf-1(ok880)* double mutant to the level of the *mec-7* or *mec-12* single mutant (Fig. 2*D*). These data indicate that *rhgf-1* functions cell-autonomously in the PLM to mediate PLM remodeling on microtubule disruption.

Expression of a RHGF-1::mCherry fusion protein revealed that RHGF-1 was distributed throughout the neuronal soma, neurites, and presynaptic varicosities of the PLM (Fig. 2*B*). Touch neuron-specific expression of the full-length RHGF-1 (FL-RHGF-1) in the wild-type at low level resulted in a small but significant reduction in the synaptic size, with rare PLM branch retraction (Fig. 2*F*). These relatively mild phenotypes of RHGF-1 overexpression could be explained by the presence of intact microtubules, which may inhibit RHGF-1 activity. Consistent with this hypothesis, low-concentration (0.125 mM) colchicine that normally caused no branch defects in otherwise wild-type animals (Fig. S1*A*) dramatically sensitized the PLM neuron to RHGF-1 expression, with 25% of the transgenic animals losing their PLM branch (Fig. 2*F*). The ability of RHGF-1 to induce branch defects was almost completely abolished by removing the DH domain. In contrast, overexpression of a RHGF-1 that contains only the DH and PH domains (DH-PH RHGF-1) resulted in a 13% and 27% branch loss without or with colchicine sensitization, respectively (Fig. 2*F*). Importantly, expression of DH-PH RHGF-1 also resulted in PLM neurite overextension (13.3%, $n = 30$), suggesting the GEF activity of RHGF-1 is necessary and sufficient for PLM remodeling on microtubule disruption.

The more robust branch retraction phenotypes caused by DH-PH RHGF-1, compared with the mild phenotypes by FL-RHGF-1 expression, suggest the N terminus of RHGF-1 inhibits its GEF activity. Consistent with this, *rhgf-1(gk217)*, which lacks the C1 domain, was very sensitive to colchicine and displayed branch defects even at a very low concentration of colchicine (Fig. 2*E*). These results indicate that the C1 domain, and possibly other domains N terminus to the DH, could inhibit DH activity. To test this hypothesis, we examined PLM branches in animals overexpressing RHGF-1 variants that lacked the PDZ, RGS, or C1 domain. We

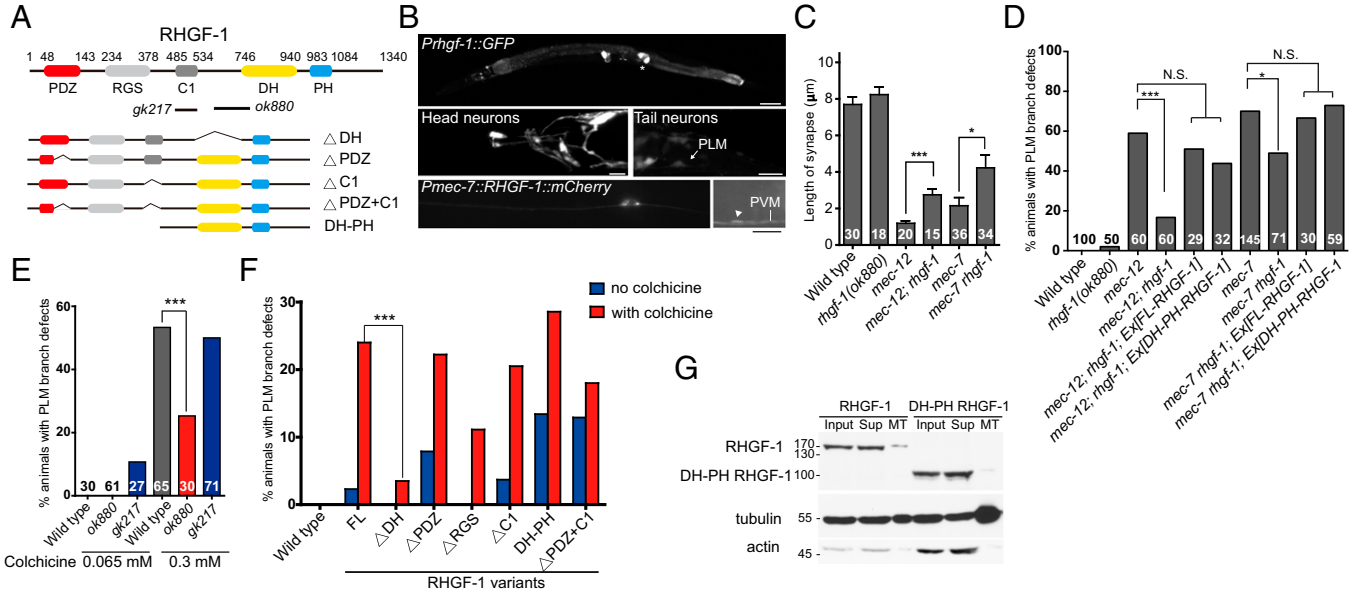

Fig. 2. RHGF-1 mediates PLM branch retraction in the tubulin mutants. (*A*) The protein structures of RHGF-1 and various RHGF-1 mutants. (*B*) (*Upper*) Confocal images of late L4 or young adult animals expressing GFP from the *rhgf-1* promoter. *rhgf-1* was expressed in the nervous system and the spermatheca (asterisks). (Scale bar, 50 μm.) (*Middle*) *rhgf-1*-expressing neurons in the head and the tail. Arrow, PLM. Anterior is to the left. (Scale bar, 10 μm.) (*Lower*) RHGF-1::mCherry in the PLM soma (*Left*) and presynaptic region (*Right*, arrowhead). (Scale bar = 10 μm.) (*C* and *D*) Quantification of the synapse length (*C*) and branch defects (*D*) in L4 larvae. $*P < 0.05$; $***P < 0.001$, Mann–Whitney *U* test ($n < 30$) or *t* test ($n > 30$) for the synapse length and two-proportion *z* test for the branch defects. N.S., not significant. (*E*) PLM branch defects with colchicine treatment in L4 larvae. (*F*) The effects of overexpressing RHGF-1 mutants on the PLM branch in the wild-type L4 larvae with or without colchicine. $*P < 0.05$; $***P < 0.001$, two-proportion *z* test. $n > 25$. (*G*) Microtubule sedimentation assay in mixed-stage animals overexpressing FL-RHGF-1 or DH-PH RHGF-1 in the nervous system. Sup, supernatant; MT, microtubule sediment.

found that the RHGF-1 that lacked both the PDZ and the C1 domains (ΔPDZ+C1) induced PLM branch defects similar to those caused by DH-PH RHGF-1 (Fig. 2*F*). This suggests that the PDZ and the C1 domains exert inhibitory effects on RHGF-1.

Mammalian PDZ-RhoGEFs had been shown to be inhibited by binding to microtubules (29). To test whether RHGF-1 binds microtubules, we expressed HA-tagged RHGF-1 in worm neurons, performed microtubule sedimentation, and assayed the amount of RHFG-1 coprecipitated with microtubules. We found that the full-length RHGF-1 coprecipitated with microtubules, but the DH-PH RHGF-1 did not (Fig. 2*G*). These data indicate that microtubules maintain axon branch stability by associating RHGF-1 through its N terminus domain and inhibiting its GEF activity. This conclusion was further supported by the colocalization of microtubules and RHGF-1 in HeLa cells, which also depended on the RHGF-1 N terminus domains (Fig. S2).

Because *rhgf-1* is broadly expressed in the *C. elegans* nervous system (27), we wonder whether inadvertent RHGF-1 activity also disrupts synapses outsides the touch receptors. Pan-neuronal DH-PH RHGF-1 expression resulted in loopy locomotion, and the animals moved with exaggerated body bends (Fig. S3*A*). At the cellular level, DH-PH RHGF-1 disrupted cholinergic motor neuron synapses in the ventral and the dorsal nerve cords (Fig. S3 *B–D*). This result indicates that the activity of RHGF-1 is not restricted to the touch neurons and could be a general mechanism that mediates synaptic and axon damage on loss of intact microtubules.

DLK-1/MAPK Functions Downstream of RHGF-1 in PLM Remodeling on Microtubule Disassembly. In a series of genetic experiments (Fig. 3*A* and Fig. S4 and *SI Results*), we demonstrated that *rhgf-1*acted through *rho-1*/Rho, *ced-10*/Rac, *mig-2*/Rac, and the Rho-dependent kinase *let-502*/ROCK to mediate PLM branch defects in the tubulin mutants, and it acted independent of the myosin light chain *mlc-4* (Fig. S4*C*). Moreover, a gain-of-function *mig-2(gm103)* mutation or expression of the constitutively active amino acid substitutions, RHO-1(G14V) or CED-10(G12V), triggered PLM branch defects (Fig. S4*A*).

Genetic or pharmacologic ablation of microtubules in *C. elegans* activates *dlk-1*, a MAPKKK (14). It had been reported that *rpm-1* mutants, which had high *dlk-1* activity, lost PLM branches (30). These observations prompted us to investigate the role of *dlk-1* in PLM branch retraction in the tubulin mutants. Indeed, we found that mutations in *dlk-1*, as well as mutations in the downstream MAPK kinase *mkk-4* and the MAPK *pmk-3*, suppressed PLM branch defects of the *mec-12* and the *mec-7* mutants (Fig. 3*B*). Our data suggest that Rho/Rac and *dlk-1* MAPK signaling functioned in a common pathway and autonomously in the PLM (Fig. 3*B* and Figs. S4*B*, S5*A*, and S6*A*), and when induced acutely with heat shock, DLK-1 could trigger PLM branch retraction in stage 4 larvae (L4) larvae (Fig. S5*B*). Remarkably, locomotion defects caused by pan-neuronal DH-PH RHGF-1 overexpression were largely suppressed by the *dlk-1* mutation (Fig. S3*A*). *dlk-1* mutations also suppressed PLM overextension in the tubulin mutants or in animals with excessive RHGF-1 activity, and overexpression of DLK-1 in the touch neurons triggered PLM branch loss and primary neurite overextension in a dose-dependent manner (Fig. 4 *A* and *B*). Although *dlk-1* transcriptional activity was not increased (Fig. S5*C*), DLK-1 protein level was higher in the tubulin mutants, suggesting microtubule disassembly leads to DLK-1 activation and stabilization (Fig. S5*D*).

DLK-1 Retrograde Signaling Contributes to PLM Branch Defects of the Tubulin Mutants. These genetic experiments confirmed DLK-1 as a major effector for PLM neuronal remodeling in response to microtubule disassembly. DLK-1 had been shown to localize to the synapses and the axons in *C. elegans* (5). We also detected a very low level of DLK-1 in the PLM soma (Fig. 4*C*). Both gene

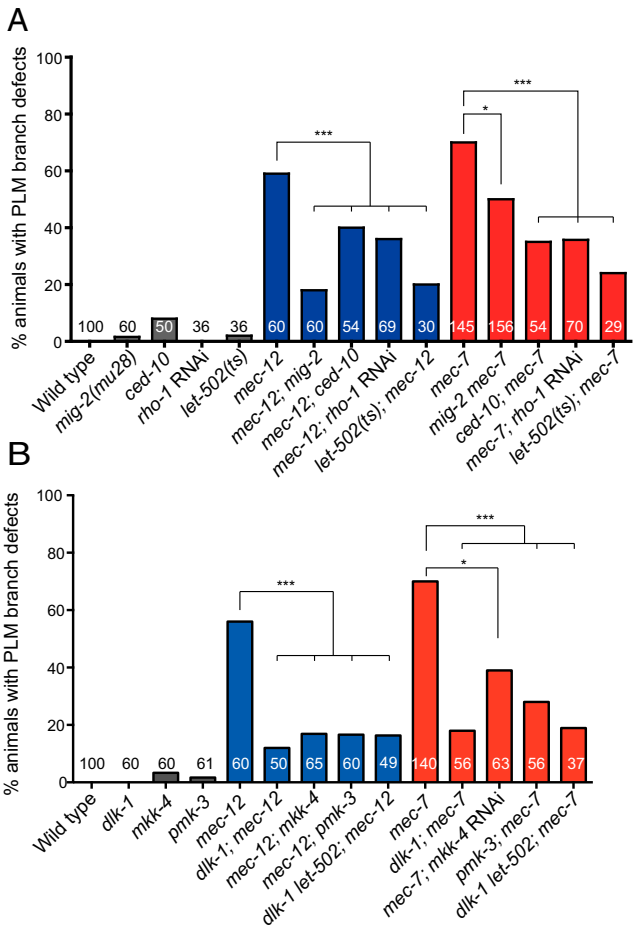

Fig. 3. Rho/Rac-ROCK (*A*) and the DLK-1 MAPK (*B*) pathways suppressed PLM branch defects of the tubulin mutants. Quantification was performed in L4 larvae in all experiments. $*P < 0.05$; $**P < 0.01$; $***P < 0.001$, two-proportion *z* test.

products, MKK-4 and PMK-3, were localized to the PLM synapse, with additional distribution in the process or the neuronal soma (Fig. 4*C*). Localization of these MAPK components to both synapses and the neuronal cell bodies suggests that active DLK-1, MKK-4, and PMK-3 function either peripherally at the synapse or centrally in the neuronal cell body. An intriguing scenario is that communication between the synaptic and somatic MAPK components initiates the neuronal remodeling.

Previous studies in fly and mice had implicated DLK-1 as an injury signal that elicits regenerative responses via retrograde axon transport (3, 31). To directly visualize DLK-1 retrograde transport, we expressed the kinase-dead DLK-1(K162A) tagged with Dendra2, which was more stable than the wild-type DLK-1 and had been used previously in *Drosophila* for similar experiments (31). Although it is a valid concern that the enzymatic activity of DLK-1 may somehow be required for its transport, it was previously shown that kinase activity was dispensable for DLK-1 dimerization (6). We first confirmed that microtubule polarity in the PLM neurite mimicked vertebrate axons, with plus ends of microtubules oriented distally (32). Our time-lapse imaging experiments showed that DLK-1(K162A) puncta moved both anterogradely and retrogradely (Fig. 4*D*) and that the retrograde DLK-1 movements were abolished by a temperature-sensitive mutation in *dhc-1*, the cytoplasmic dynein heavy chain (33–35) (Fig. 4*D*). Anterograde DLK-1 movements were also decreased in the *dhc-1* mutant, possibly because kinesins in the neuronal soma were replenished via

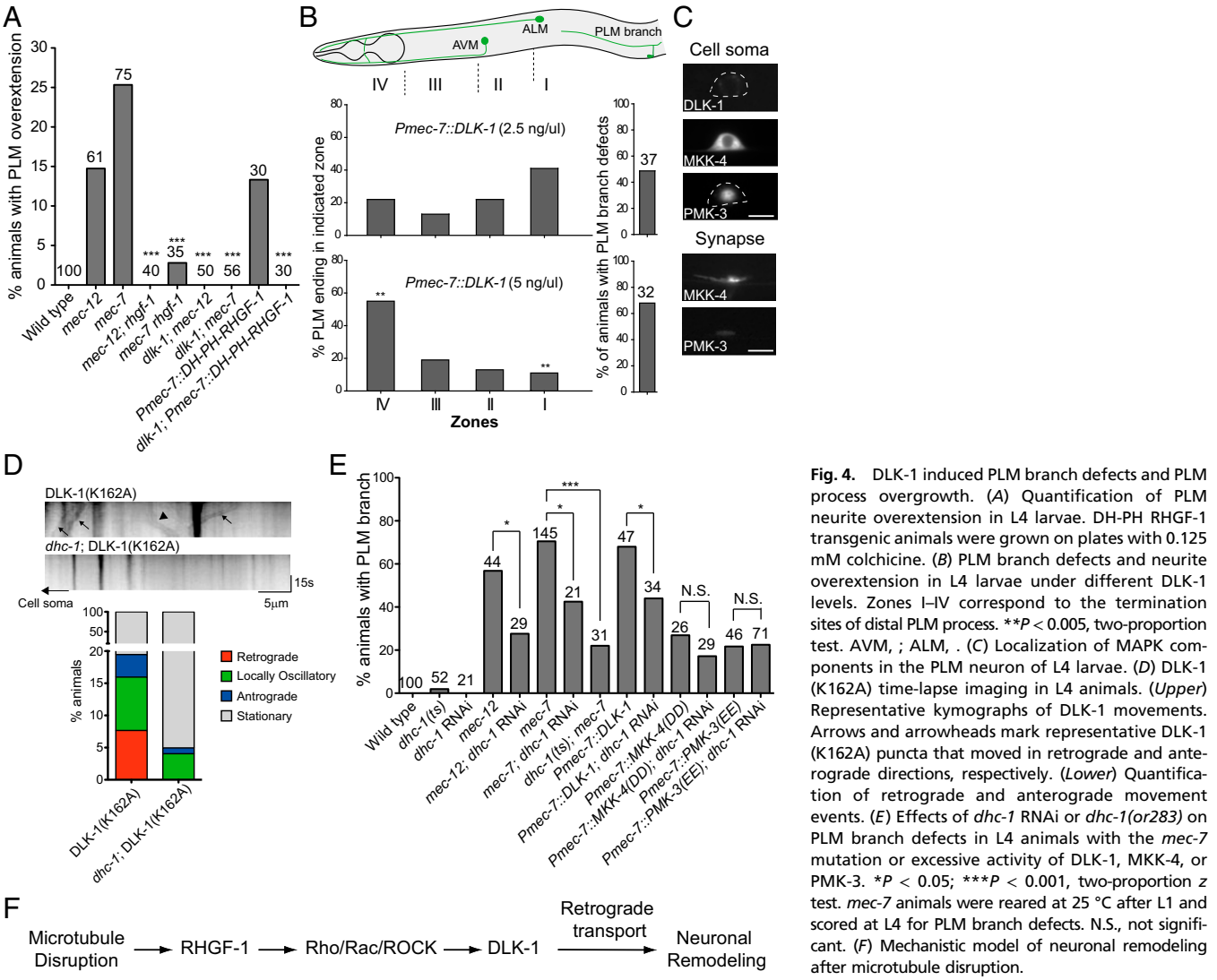

Fig. 4. DLK-1 induced PLM branch defects and PLM process overgrowth. (*A*) Quantification of PLM neurite overextension in L4 larvae. DH-PH RHGF-1 transgenic animals were grown on plates with 0.125 mM colchicine. (*B*) PLM branch defects and neurite overextension in L4 larvae under different DLK-1 levels. Zones I–IV correspond to the termination sites of distal PLM process. $^{**}P < 0.005$, two-proportion test. AVM, ; ALM, . (*C*) Localization of MAPK components in the PLM neuron of L4 larvae. (*D*) DLK-1 (K162A) time-lapse imaging in L4 animals. (*Upper*) Representative kymographs of DLK-1 movements. Arrows and arrowheads mark representative DLK-1 (K162A) puncta that moved in retrograde and anterograde directions, respectively. (*Lower*) Quantification of retrograde and anterograde movement events. (*E*) Effects of *dhc-1* RNAi or *dhc-1(or283)* on PLM branch defects in L4 animals with the *mec-7* mutation or excessive activity of DLK-1, MKK-4, or PMK-3. $^{*}P < 0.05$; $^{***}P < 0.001$, two-proportion *z* test. *mec-7* animals were reared at 25 °C after L1 and scored at L4 for PLM branch defects. N.S., not significant. (*F*) Mechanistic model of neuronal remodeling after microtubule disruption.

dynein-dependent retrograde transport. Imaging of MKK-4 or PMK-3 movements in the PLM neurite was not possible because of their diffuse, nonpunctual distribution.

Having established DLK-1 retrograde transport in the *C. elegans* PLM neurite, we tested whether elimination of *dhc-1* ameliorates PLM branch defects caused by MAPK activation. We achieved cell-specific *dhc-1* RNAi by simultaneously expressing the sense and antisense *dhc-1* RNA from the *mec-7* promoter (transgenic *dhc-1* RNAi; *SI Materials and Methods*). *dhc-1* RNAi markedly attenuated PLM branch defects caused by DLK-1 overexpression (Fig. 4*E*), although it did not significantly reduce PLM branch defects caused by overexpression of the phosphomimetic, active MKK-4 or PMK-3 (Fig. 4*E*). Moreover, both transgenic *dhc-1* RNAi and the temperature-sensitive *dhc-1(or283)* mutation significantly suppressed PLM branch defects of the *mec-7* mutant (Fig. 4*E*). These data support a model (Fig. 4*F*) that on microtubule disruption, active DLK-1 triggered by RHGF-1 released from the microtubules-based inhibition was retrogradely transported to the neuronal soma and activated MKK-4 and PMK-3 in the cytoplasm to induce PLM remodeling. Experiments further suggest that *rpm-1* is part of this pathway and likely acts downstream of Rho/Rac/ROCK signaling, but upstream of *dlk-1* (Figs. 4*F* and Fig. S5*D*). Considering the variability of RNAi expressed in the form of extrachromosomal arrays, we cannot complete rule out that MKK-4 or PMK-3 may also signal retrogradely in a dynein-dependent fashion. Unfortunately, available *dhc-1* temperature-sensitive alleles failed to survive upshift to restrictive temperature in embryogenesis, which is necessary to interfere with the MKK-4 and PMK-3 functions that begin before the animals hatch. Additional genetic tools are necessary to test definitely the role of MKK-4 and PMK-3 in retrograde DLK-1 signaling.

Discussion

Our observations suggest a neuronal remodeling paradigm during *C. elegans* development that reorganizes the touch neuronal circuit by the coordinated removal of the dysfunctional synaptic compartment and compensatory growth of the primary process. In this work, we identified RHGF-1 as a major factor that induces structural remodeling when neuronal microtubules are disrupted. RHGF-1 activation triggers synaptic and axon branch retraction and excessive extension of the primary neurite, all through the conserved remodeling effector DLK-1. The finding that RHGF-1 is normally associated with and inhibited by microtubules makes RHGF-1 an ideal sensor that monitors microtubule integrity, with its remodeling activity fine-tuned by the degree of microtubule disassembly. Of note, this function of *rhgf-1* is distinct from its role as a regulator of neurotransmitter release at the cholinergic motor synapses that depends on G protein signaling (26).

Two studies of the *C. elegans* PTRN-1/CAMSAP suggest this microtubule minus end-binding protein maintains synapse and neurite stability (12, 13). The *ptrn-1* mutant showed PLM remodeling phenotypes remarkably similar to those of the *mec-12* and *mec-7* tubulin mutants, highlighting the importance of the microtubule as a central regulator of structural stability and plasticity of the neuronal circuit. Interestingly, neuronal remodeling in the *ptrn-1* mutant also depended on *dlk-1*, which had been implicated in both Wallerian degeneration and axon regeneration (1, 2, 4, 36). In these studies, it was not clear how *dlk-1* was activated on microtubule disruption in the developmental (the *ptrn-1* cases) or post-developmental (the axon injury models) contexts. Our data suggest that RHGF-1 may function through the LET-502/ROCK as a proxy for microtubule perturbation to activate DLK-1. Because the substrate (microtubule), the sensor (RHGF-1), and the effector (DLK) are conserved, we hypothesize that this neuronal remodeling paradigm could be a shared feature of the nervous system in different organisms.

DLK activates transcription of both apoptotic and regenerative genes in mammalian neurons (37). In the tubulin mutants, overextension of the primary neurite paralleled elimination of the synaptic branch. It is possible that compartment-specific DLK regulators are involved in mediating distinct DLK effects in different subcellular compartments. A future challenge is the identification of molecules that act in a compartment-specific way to coordinate synaptic or branch maintenance and axon regeneration.

Experimental Procedures

***C. elegans* Strains and Genetics.** Strains were cultured and maintained as described (38). All alleles and transgenes used in this study are available online in *Supporting Information*.

Microtubule Sedimentation Assay. The microtubule sedimentation assay was performed as described, with modifications (39). In brief, unc-119; twnEx187 [Punc-119::FL-RHGF-1::HA, Punc-119::mec-12, Punc-119::mec-7, unc-119(+)] and unc-119; twnEx188[Punc-119::DH-PH RHGF-1::HA, Punc-119::mec-12, Punc-119::mec-7, unc-119(+)] transgenic animals were collected in 0.1 M Pipes (pH 6.94), 4.0 mM $MgCl_2$, 5 mM EGTA, 0.1 mM EDTA, 0.9 M glycerol, 1 mM PMSF, and 1 mM DTT (PMEG) at 4 °C and resuspended in cold PMEG with protease inhibitor. Worms were manually homogenized and centrifuged at 20,000 × *g* for 45 min, the supernatant was further centrifuged at 150,000 × *g* for 60 min, and the pellet was discarded. The translucent supernatant was added with 2 mM GTP, 10 pM taxol, 1 U/mL hexokinase, 50 mM glucose, and 25–50 nm AMP-PNP and incubated on ice for 90 min for microtubule polymerization. Microtubules were sedimented through 20% (vol/vol) sucrose cushion in PMEG with 10 pM taxol by centrifugation at 20,000 × *g* for 90 min. The pellet was resuspended in 1 mL PMEG with 10 nM taxol and 50 mM NaCl. Microtubules and associated proteins were pelleted at 20,000 × *g* for 40 min and dissolved in water for further analysis.

ACKNOWLEDGMENTS. We thank Martin Chalfie, James Ervasti, Gian Garriga, Josh Kaplan, Erik Lundquist, Paul Mains, Kunihiro Matsumoto, Michael Nonet, Stephen Nurrish, and Yi-Chun Wu for strains and reagents. We thank Gian Garriga, Jason Chien, and Hwai-Jong Cheng for comments on the manuscript. Some strains were provided by the *C. elegans* Genetics Center, which is funded by National Institutes of Health Office of Research Infrastructure Programs (P40 OD010440), and by the National BioResources Project, Japan. This study was funded by the National Science Council (NSC99-2320-B-002-080 and NSC100-2320-B-002-095-MY3 to C.-L.P. and NSC101-2321-B-002-071-MY3 to Y.-W.L.) and by the National Taiwan University (NTU-CDP-102R7810 to C.-L.P.).

1. Hammarlund M, Nix P, Hauth L, Jorgensen EM, Bastiani M (2009) Axon regeneration requires a conserved MAP kinase pathway. *Science* 323(5915):802–806.
2. Miller BR, et al. (2009) A dual leucine kinase-dependent axon self-destruction program promotes Wallerian degeneration. *Nat Neurosci* 12(4):387–389.
3. Shin JE, et al. (2012) Dual leucine zipper kinase is required for retrograde injury signaling and axonal regeneration. *Neuron* 74(6):1015–1022.
4. Yan D, Wu Z, Chisholm AD, Jin Y (2009) The DLK-1 kinase promotes mRNA stability and local translation in *C. elegans* synapses and axon regeneration. *Cell* 138(5):1005–1018.
5. Nakata K, et al. (2005) Regulation of a DLK-1 and p38 MAP kinase pathway by the ubiquitin ligase RPM-1 is required for presynaptic development. *Cell* 120(3):407–420.
6. Yan D, Jin Y (2012) Regulation of DLK-1 kinase activity by calcium-mediated dissociation from an inhibitory isoform. *Neuron* 76(3):534–548.
7. Byrne AB, et al. (2014) Insulin/IGF1 signaling inhibits age-dependent axon regeneration. *Neuron* 81(3):561–573.
8. Conde C, Cáceres A (2009) Microtubule assembly, organization and dynamics in axons and dendrites. *Nat Rev Neurosci* 10(5):319–332.
9. Goellner B, Aberle H (2012) The synaptic cytoskeleton in development and disease. *Dev Neurobiol* 72(1):111–125.
10. Pielage J, et al. (2008) A presynaptic giant ankyrin stabilizes the NMJ through regulation of presynaptic microtubules and transsynaptic cell adhesion. *Neuron* 58(2):195–209.
11. Pielage J, Fetter RD, Davis GW (2005) Presynaptic spectrin is essential for synapse stabilization. *Curr Biol* 15(10):918–928.
12. Marcette JD, Chen JJ, Nonet ML (2014) The *Caenorhabditis elegans* microtubule minus-end binding homolog PTRN-1 stabilizes synapses and neurites. *eLife* 3:e01637.
13. Richardson CE, et al. (2014) PTRN-1, a microtubule minus end-binding CAMSAP homolog, promotes microtubule function in *Caenorhabditis elegans* neurons. *eLife* 3:e01498.
14. Bounoutas A, et al. (2011) Microtubule depolymerization in *Caenorhabditis elegans* touch receptor neurons reduces gene expression through a p38 MAPK pathway. *Proc Natl Acad Sci USA* 108(10):3982–3987.
15. Chia PH, Patel MR, Shen K (2012) NAB-1 instructs synapse assembly by linking adhesion molecules and F-actin to active zone proteins. *Nat Neurosci* 15(2):234–242.
16. Chalfie M, et al. (1985) The neural circuit for touch sensitivity in *Caenorhabditis elegans*. *J Neurosci* 5(4):956–964.
17. Chalfie M, Sulston J (1981) Developmental genetics of the mechanosensory neurons of *Caenorhabditis elegans*. *Dev Biol* 82(2):358–370.
18. Fukushige T, et al. (1999) MEC-12, an alpha-tubulin required for touch sensitivity in *C. elegans*. *J Cell Sci* 112(Pt 3):395–403.
19. Savage C, et al. (1994) Mutations in the *Caenorhabditis elegans* beta-tubulin gene *mec-7*: Effects on microtubule assembly and stability and on tubulin autoregulation. *J Cell Sci* 107(Pt 8):2165–2175.
20. Gallegos ME, Bargmann CI (2004) Mechanosensory neurite termination and tiling depend on SAX-2 and the SAX-1 kinase. *Neuron* 44(2):239–249.
21. Enomoto T (1996) Microtubule disruption induces the formation of actin stress fibers and focal adhesions in cultured cells: Possible involvement of the rho signal cascade. *Cell Struct Funct* 21(5):317–326.
22. Ren XD, Kiosses WB, Schwartz MA (1999) Regulation of the small GTP-binding protein Rho by cell adhesion and the cytoskeleton. *EMBO J* 18(3):578–585.
23. Billuart P, Winter CG, Maresh A, Zhao X, Luo L (2001) Regulating axon branch stability: The role of p190 RhoGAP in repressing a retraction signaling pathway. *Cell* 107(2):195–207.
24. Calixto A, Chelur D, Topalidou I, Chen X, Chalfie M (2010) Enhanced neuronal RNAi in *C. elegans* using SID-1. *Nat Methods* 7(7):554–559.
25. Ziel JW, Matus DQ, Sherwood DR (2009) An expression screen for RhoGEF genes involved in *C. elegans* gonadogenesis. *Gene Expr Patterns* 9(6):397–403.
26. Hiley E, McMullan R, Nurrish SJ (2006) The Galpha12-RGS RhoGEF-RhoA signalling pathway regulates neurotransmitter release in *C. elegans*. *EMBO J* 25(24):5884–5895.
27. Yau DM, et al. (2003) Identification and molecular characterization of the G alpha12-Rho guanine nucleotide exchange factor pathway in *Caenorhabditis elegans*. *Proc Natl Acad Sci USA* 100(25):14748–14753.
28. Lin L, et al. (2012) RHGF-2 is an essential Rho-1 specific RhoGEF that binds to the multi-PDZ domain scaffold protein MPZ-1 in *Caenorhabditis elegans*. *PLoS ONE* 7(2):e31499.
29. Longhurst DM, Watanabe M, Rothstein JD, Jackson M (2006) Interaction of PDZRhoGEF with microtubule-associated protein 1 light chains: Link between microtubules, actin cytoskeleton, and neuronal polarity. *J Biol Chem* 281(17):12030–12040.
30. Grill B, et al. (2007) *C. elegans* RPM-1 regulates axon termination and synaptogenesis through the Rab GEF GLO-4 and the Rab GTPase GLO-1. *Neuron* 55(4):587–601.
31. Xiong X, et al. (2010) Protein turnover of the Wallenda/DLK kinase regulates a retrograde response to axonal injury. *J Cell Biol* 191(1):211–223.
32. Ghosh-Roy A, Goncharov A, Jin Y, Chisholm AD (2012) Kinesin-13 and tubulin post-translational modifications regulate microtubule growth in axon regeneration. *Dev Cell* 23(4):716–728.
33. Gönczy P, Pichler S, Kirkham M, Hyman AA (1999) Cytoplasmic dynein is required for distinct aspects of MTOC positioning, including centrosome separation, in the one cell stage *Caenorhabditis elegans* embryo. *J Cell Biol* 147(1):135–150.
34. Koushika SP, et al. (2004) Mutations in *Caenorhabditis elegans* cytoplasmic dynein components reveal specificity of neuronal retrograde cargo. *J Neurosci* 24(16):3907–3916.
35. O'Rourke SM, Dorfman MD, Carter JC, Bowerman B (2007) Dynein modifiers in *C. elegans*: Light chains suppress conditional heavy chain mutants. *PLoS Genet* 3(8):e128.
36. Xiong X, Collins CA (2012) A conditioning lesion protects axons from degeneration via the Wallenda/DLK MAP kinase signaling cascade. *J Neurosci* 32(2):610–615.
37. Watkins TA, et al. (2013) DLK initiates a transcriptional program that couples apoptotic and regenerative responses to axonal injury. *Proc Natl Acad Sci USA* 110(10):4039–4044.
38. Brenner S (1974) The genetics of *Caenorhabditis elegans*. *Genetics* 77(1):71–94.
39. Lye RJ, Porter ME, Scholey JM, McIntosh JR (1987) Identification of a microtubule-based cytoplasmic motor in the nematode *C. elegans*. *Cell* 51(2):309–318.